

Journal of Geophysical Research: Earth Surface

RESEARCH ARTICLE

10.1002/2013JF002931

Key Points:

- In regions with large glacier volume loss, runoff declines over the next century
- In other regions runoff will increase throughout the century or peak mid-century
- Glacier net mass loss is a significant percentage of total glacier runoff

Correspondence to:

A. Bliss,
andybliss@gmail.com

Citation:

Bliss, A., R. Hock, and V. Radić (2014), Global response of glacier runoff to twenty-first century climate change, *J. Geophys. Res. Earth Surf.*, 119, 717–730, doi:10.1002/2013JF002931.

Received 23 JUL 2013

Accepted 7 FEB 2014

Accepted article online 12 FEB 2014

Published online 1 APR 2014

Global response of glacier runoff to twenty-first century climate change

Andrew Bliss¹, Regine Hock^{1,2}, and Valentina Radic³

¹Geophysical Institute, University of Alaska Fairbanks, Fairbanks, Alaska, USA, ²Department of Earth Sciences, Uppsala University, Uppsala, Sweden, ³Department of Earth and Ocean Sciences, University of British Columbia, Vancouver, British Columbia, Canada

Abstract The hydrology of many important river systems in the world is influenced by the presence of glaciers in their upper reaches. We assess the global-scale response of glacier runoff to climate change, where glacier runoff is defined as all melt and rain water that runs off the glacierized area without refreezing. With an elevation-dependent glacier mass balance model, we project monthly glacier runoff for all mountain glaciers and ice caps outside Antarctica until 2100 using temperature and precipitation scenarios from 14 global climate models. We aggregate results for 18 glacierized regions. Despite continuous glacier net mass loss in all regions, trends in annual glacier runoff differ significantly among regions depending on the balance between increased glacier melt and reduction in glacier storage as glaciers shrink. While most regions show significant negative runoff trends, some regions exhibit steady increases in runoff (Canadian and Russian Arctic), or increases followed by decreases (Svalbard and Iceland). Annual glacier runoff is dominated by melt in most regions, but rain is a major contributor in the monsoon-affected regions of Asia and maritime regions such as New Zealand and Iceland. Annual net glacier mass loss dominates total glacier melt especially in some high-latitude regions, while seasonal melt is dominant in wetter climate regimes. Our results highlight the variety of glacier runoff responses to climate change and the need to include glacier net mass loss in assessments of future hydrological change.

1. Introduction

Glaciers store and release water on a range of time scales [Jansson *et al.*, 2003] and therefore can significantly modify river runoff regimes [Hock *et al.*, 2005]. On annual time scales, glaciers contribute additional water to rivers when glacier mass balances are negative, while reducing river flow in case of glacier mass gain. On shorter time scales, glaciers modify runoff regimes by releasing most of the annual meltwater during the summer months, which is often a period of otherwise low flow conditions. Worldwide glacier mass loss and retreat [Gardner *et al.*, 2013] and projected accelerated future mass losses [Marzeion *et al.*, 2012; Radic *et al.*, 2013] raise concerns about the sustainability of water supplies and resulting socioeconomic implications. As glaciers melt at a faster rate due to atmospheric warming, they will provide increased water to downstream reaches. However, this will be followed by a reduction in runoff as the glaciers dwindle [Jansson *et al.*, 2003]. The initial increase in glacier runoff can be substantial, strongly exceeding the runoff changes to be expected from any other component of the glacier's water budget. In the longer term, glacier retreat will cause a reduction in total runoff, potentially affecting water resource availability. Changes in the proportion of streamflow originating from glaciers will also impact the physical, biogeochemical [Hood and Berner, 2009], and biological [Robinson *et al.*, 2001] properties of streams due to significantly different characteristics compared to nonglacier derived water sources.

While most studies on glacier runoff have focused on individual glacierized catchments or glaciers [Huss *et al.*, 2008; Koboltschnig *et al.*, 2008; Stahl *et al.*, 2008; Immerzeel *et al.*, 2010; Farinotti *et al.*, 2012], few studies have investigated the hydrological consequences of changing glaciers on regional or global scales. Dyurgerov [2010] compared river discharge from gauging stations to estimates of meltwater fluxes and annual mass changes of all glaciers draining to the Arctic Ocean including the Greenland ice sheet and concluded that the glaciers play an important role in Arctic freshwater budgets. Using a water balance approach, Neal *et al.* [2010] found that runoff from the ice-covered part of the drainage basin (18% of 420,230 km²) contributed 47% of the total runoff to the Gulf of Alaska. Ten percent originated from glacier net mass loss alone. Huss [2011] compared monthly glacier runoff, defined as the water lost due to glacier mass change for each month, to monthly river runoff measured at gauges along the entire river lengths of some of the largest

European rivers and concluded that seasonal contributions from glaciers can be significant even in large-scale watersheds with less than 1% ice cover. Comeau *et al.* [2009] and Weber *et al.* [2010] used hydrological modeling to quantify the contribution of glaciers to runoff in large river basins in Canada and Central Europe, respectively. Kaser *et al.* [2010] assessed the effect of glaciers on runoff by computing the fraction of runoff that is seasonally delayed by glaciers for 18 large river basins around the world. Combined with a population index to assess the societal impact of delayed runoff they found significant differences in the importance of glaciers on runoff depending on climate regime, with most significant impacts in seasonally arid regions and negligible effects in monsoon climates. Gardelle *et al.* [2013] used DEM differencing to show that within river basins in High Mountain Asia, net glacier mass loss can be larger than the seasonal melt reported in Kaser *et al.* [2010].

Several recent studies have modeled twenty-first century glacier mass changes in response to climate scenarios [Radić and Hock, 2011; Marzeion *et al.*, 2012; Giesen and Oerlemans, 2013; Radić *et al.*, 2013]. However, the evolution of regional to global scale changes in glacier runoff has not been addressed by these modeling efforts. The purpose of this study is to assess, on a global scale, the changes in glacier runoff to be expected until 2100 in response to transient climate scenarios. We use a temperature-index mass-balance model to project monthly glacier runoff from all mountain glaciers and ice caps in the world (excluding those in the Antarctic periphery) for the twenty-first century forced by temperature and precipitation scenarios from 14 Global Climate Models (GCMs). Results are aggregated for 18 glacierized regions and analyzed with respect to changes in annual total runoff, the proportion of glacier runoff due to glacier melt, net mass loss and liquid precipitation, and changes in runoff regime and runoff trends.

2. Definition of Glacier Runoff

Here we take a water balance approach and compute monthly and annual runoff totals Q_g from the glacierized area with

$$Q_g = M - R + P_l, \quad (1)$$

where M is melt of ice, firn, and snow; R is refreezing; and P_l is liquid precipitation. We assume evaporation, sublimation, and any storage changes (groundwater, englacial, or subglacial) to be negligible compared to the other terms [Huss *et al.*, 2008]. All quantities are integrated over an annually updated glacier area. Since this area evolves with time, as the glacier retreats or advances, we effectively model the glacier discharge that would be measured by an imaginary gauging station that moves with the position of the terminus. This allows us to precisely track the unique chemical and physical properties associated with glacier runoff, as distinct from runoff from other surface types. Models that use a fixed watershed rather than a moving gauge may have greater utility for water resource managers and people who live near glaciers, since people draw water from a fixed location rather than from the glacier directly. It is also easier to interpret changes to the seasonality of runoff when looking at data from a fixed gauge location. However, fixed watershed models must include additional parameters governing precipitation, snow melt, and water transport over unglacierized areas that cannot be calibrated with the data sets we use here.

To evaluate in how far glacier wastage contributes to annual runoff, we distinguish two components of total melt M :

$$M = M_{\Delta V} + M_{\text{seas}} \quad (2)$$

where $M_{\Delta V}$ is melt water from annual glacier net mass loss and M_{seas} is the component of annual total melt that does not contribute to net glacier mass loss, here referred to as seasonal melt. $M_{\Delta V}$ is derived from the climatic glacier mass balance B_{clim} :

$$M_{\Delta V} = -\min(0, B_{\text{clim}}). \quad (3)$$

$$B_{\text{clim}} = C - A + R, \quad (4)$$

where C is accumulation (here snowfall), A is ablation, and R is refreezing. We neglect any form of mass loss other than surface melt, so $A = M$. The climatic glacier mass balance only contributes to glacier runoff if there is a net mass loss ($B_{\text{clim}} < 0$); in case of a balanced or positive mass budget, $M_{\Delta V} = 0$, and annual total melt is equivalent to seasonal melt, $M = M_{\text{seas}}$. In case of a negative mass budget, M_{seas} corresponds to the melt a glacier would have under hypothetical balanced budget conditions: $M_{\text{seas}} = C + R$. Due to typical mass balance profiles, with net mass gains in the accumulation area and net mass losses in the ablation area, M_{seas} includes not only melt of seasonal snow but also melt of glacier ice in the ablation area.

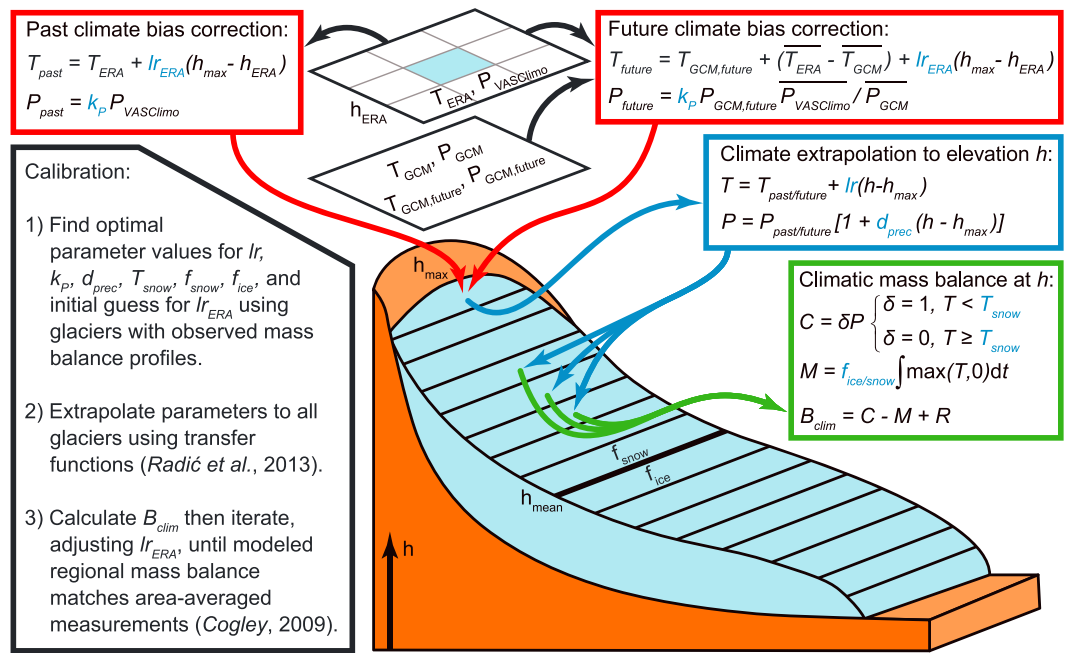


Figure 1. Schematic illustration of the model that derives climatic mass balance B_{clim} for each elevation band on a glacier. T is monthly mean air temperature, and P is monthly precipitation. Overbar symbols represent average monthly values over the period 1980–1999. Tuneable model parameters are in blue print: lr_{ERA} , ‘statistical’ temperature lapse rate (used to estimate the temperature at the top glacier elevation, h_{max} , from ERA-40 temperature at the altitude of the grid cell containing the glacier); lr , temperature lapse rate along the glacier; k_p , precipitation correction factor (to estimate the precipitation at the top of the glacier from the VASClimo precipitation for the grid cell containing the glacier); d_{prec} , precipitation gradient along the glacier; T_{snow} threshold temperature used to discriminate snow from rain precipitation; f_{ice} , degree-day factor for ice (applied where $h < h_{mean}$, the mean glacier elevation); and f_{snow} degree day factor for snow ($h > h_{mean}$). C is accumulation, M is melt, and R is refreezing (after Woodward et al., 1997).

3. Methods

3.1. Model Description

We use a model that has been developed for global-scale mass-balance calculations and applied to project the volume evolution of all glaciers outside the Antarctic and Greenlandic ice sheets until 2100 [Radić and Hock, 2011; Radić et al., 2013]. Figure 1 illustrates the model equations and parameters. The model is forced by monthly mean near-surface air temperatures and monthly precipitation totals from gridded climate data and calculates snow accumulation, melt, and refreezing for each elevation band of each glacier. Snow accumulation is calculated from precipitation modified by a correction factor and a precipitation gradient along the glacier, and using a near-surface air temperature threshold to distinguish between rain and snowfall. A degree-day approach is used to model melt using different degree-day factors for snow/firn and ice and a temperature lapse rate to distribute air temperatures across the glacier. Following Woodward et al. [1997], refreezing is computed from potential refreezing depths approximated as a function of annual mean near-surface air temperature. To capture the feedback between glacier mass balance and changing glacier extent, the glacier’s length and area-altitude distribution are adjusted at the end of each mass-balance year using volume-length scaling [Bahr et al., 1997; Radić and Hock, 2006; Radić et al., 2008]. Glacier thickness changes are not accounted for, except within the elevation bands subject to retreat or advance. The individual steps involved in coupling the surface mass balance modeling with volume-length scaling are illustrated schematically in Figure 2. Radić et al. [2008] demonstrated that the scaling method produces volume evolutions of individual glaciers similar to those derived from a flowline model. Furthermore, Adhikari and Marshall [2012] showed that glacier volumes generated from volume-area scaling (using parameters similar to the ones we use) matched volumes generated by a 3-D Stokes model. However, Radić et al. [2008] also showed that the application of scaling is deficient for deriving absolute glacier volume and absolute volume changes of individual glaciers and should only be considered reliable when applied on a large sample

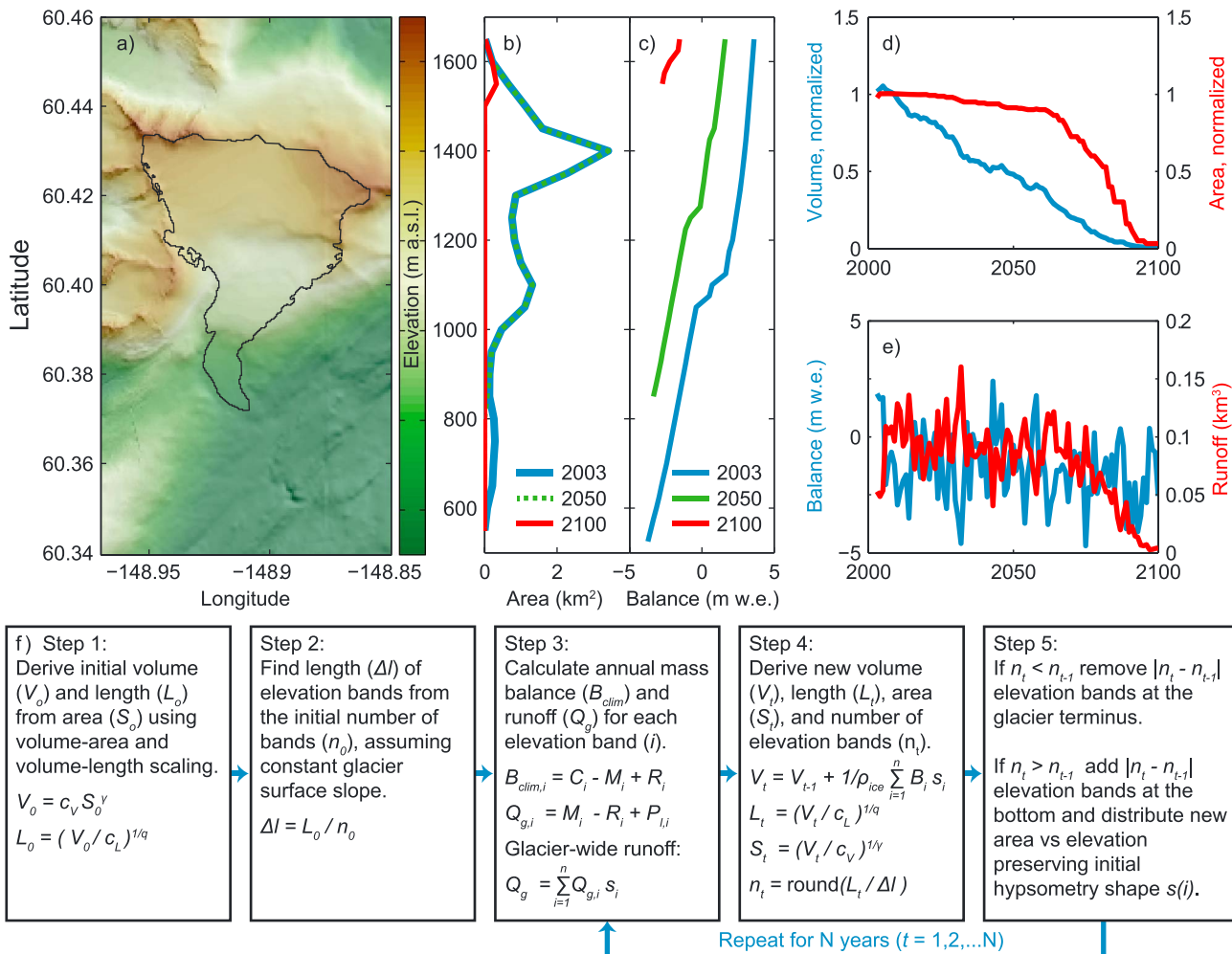


Figure 2. Schematic illustration of model steps. (a) Example of a glacier outline from the Randolph Glacier Inventory and topography from a digital elevation model. (b) Area-altitude distribution. (c) Modeled annual climatic mass balance B_{clim} versus elevation h for the sample glacier. (d) Time series of annual glacier volume and area, normalized to their initial values. (e) Time series of annual glacier-wide B_{clim} and glacier runoff. (f) Flowchart of the individual steps involved in coupling the surface mass balance model with the length scaling. Parameter values in the scaling relationships used for mountain glaciers are $c_V = 0.2055 \text{ m}^{3-2\gamma}$, $\gamma = 1.375$, $c_L = 4.5507 \text{ m}^{3-q}$, $q = 2.2$, while the parameter values for ice caps are $c_V = 1.7026 \text{ m}^{3-2\gamma}$, $\gamma = 1.250$, $c_L = 7.1209 \text{ m}^{3-q}$, $q = 0.4$. See equations (1)–(4) for variables C , M , R , and Q_g . ρ_{ice} is ice density (assumed to be 900 kg m^{-3}).

of glaciers owing to statistical effect of bias cancellation [Bahr *et al.*, 1997; Meier *et al.*, 2007]. Therefore, we integrate absolute volume changes and glacier runoff totals over a large suite of glaciers, i.e., as regional volume and runoff changes, with hundreds of glaciers per region. If a constant glacier area is assumed instead of allowing the glacier geometry to change, volume losses can be overestimated by 20% or more [Radić *et al.*, 2008].

To calibrate the mass balance model, Radić *et al.* [2013] used monthly temperatures from ERA-40 and precipitation data from the VASClimeO project [Beck *et al.*, 2005]. Seven model parameters (listed in blue in Figure 1) were calibrated, maximizing the agreement between simulations and observations, for a sample of 36 glaciers with observations of seasonal mass balance profiles [Radić and Hock, 2011]. Parameter values for all modeled glaciers were then derived from empirical relationships between the calibrated model parameters and climatic variables, and where significant relations could not be found, from adopting the mean value from the sample of 36 calibration glaciers. In a final calibration step, the ‘statistical’ temperature lapse rate (βr_{ERA} Figure 1) was tuned to minimize the misfit between the model and 1961–2000 time series of subregional area-weighted climatic mass balances estimated from glaciological records by Cogley [2009]. This final tuning procedure was necessary to initialize the modeled mass balances on regional scale prior to future projections.

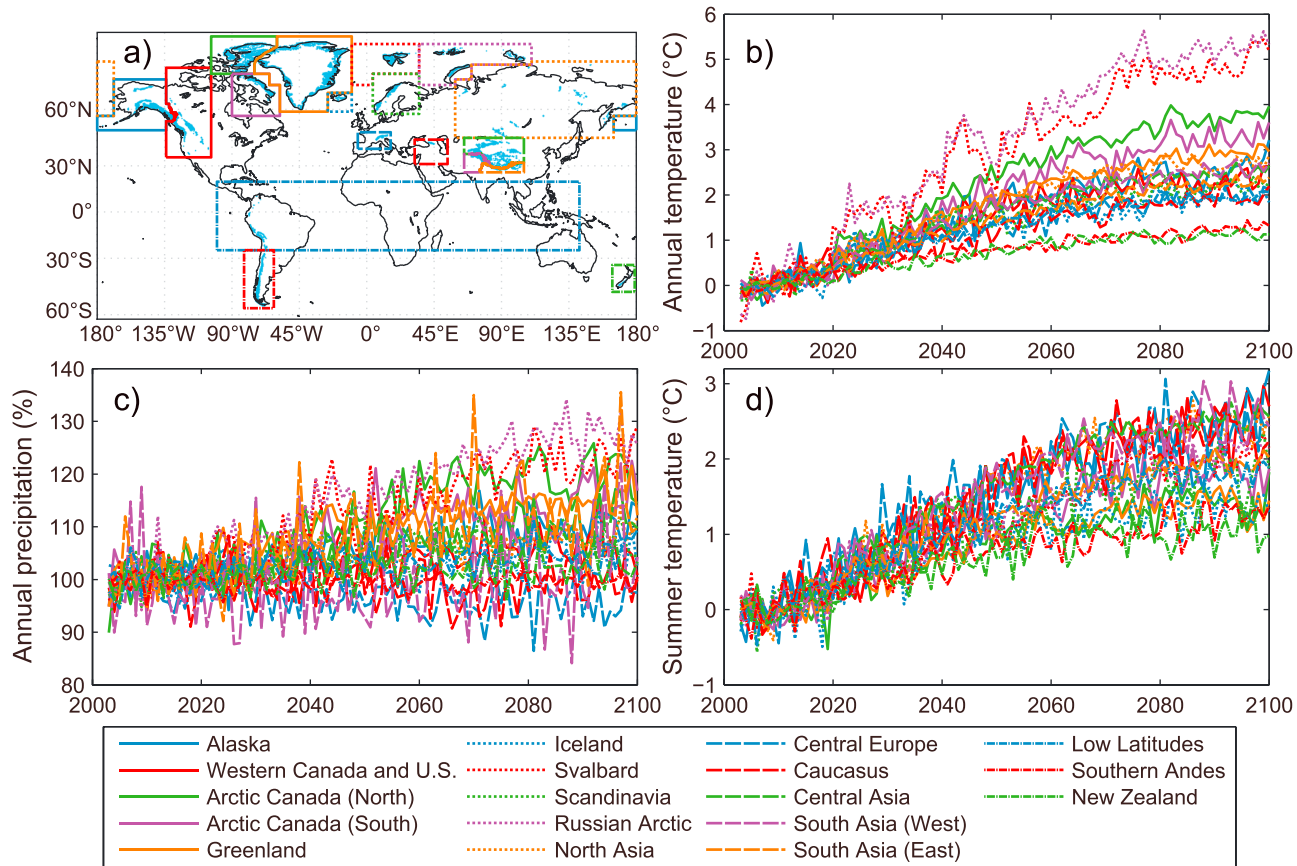


Figure 3. (a) Location map of glaciers (light blue dots) and region boundaries (colored lines). Anomalies of (b) annual mean temperature, (c) annual precipitation, and (d) summer temperature (June–August for Northern Hemisphere and December–February for Southern Hemisphere). $T_{\text{anomaly}} = T - \langle T \rangle$ and $P_{\text{anomaly}} = P / \langle P \rangle$ where $\langle \cdot \rangle$ denotes the mean for 2003–2012. Time series are multimodel means, from 14 GCMs with the RCP4.5 emission scenario, averaged over all GCM grid cells in a region, weighted by the 2003 glacier area within each cell.

For the projections of glacier volume, Radić *et al.* [2013] used the runs of 14 GCMs, selected from Coupled Model Intercomparison Project Phase 5 (CMIP5), based on two emission scenarios referred to as Representative Concentration Pathways [Moss *et al.*, 2010]: RCP4.5 and RCP8.5. The labels for the RCPs provide a rough estimate of the radiative forcing in the year 2100 relative to the preindustrial conditions (e.g., RCP4.5 reaches a level of about 4.5 W m^{-2} by 2100). Prior to the mass balance modeling, the monthly near-surface air temperature from each GCM was adjusted (Figure 1) to correct for the mean bias for each month between the GCM historical run and ERA-40 temperatures over the period 1980–1999. For precipitation, a mean monthly correction factor between the GCM and the VASClmO climatology was applied to the GCM output. More detailed information about the model, calibration procedure, projections, and uncertainties is given in Radić and Hock [2011] and Radić *et al.* [2013].

3.2. Model Application

Here we use the same input data, calibrated model parameters, and model setup as in Radić *et al.* [2013], but instead of glacier volume and mass balance, we output the glacier runoff and individual components of the water balance as defined by equation (1). Because the model is calibrated to capture the seasonality of glacier mass balance [Radić *et al.*, 2013] rather than just annual values, we consider the model sufficiently robust to simulate monthly, in addition to annual glacier runoff. The model is applied to all glaciers of the Randolph Glacier Inventory (RGI, Version 2.0) [Arendt *et al.*, 2012; W. Pfeffer *et al.*, The Randolph Glacier Inventory: A globally complete inventory of glaciers, submitted to *Journal of Glaciology*, 2014], with the exception of those in the Antarctic periphery; in total there are 197,543 glaciers covering 604,122 km². Model output is compiled for 18 regions consistent with the RGI regions (Figure 3). Following Radić *et al.* [2013], we force the model with monthly near surface (2 m) temperature and precipitation output from 14 GCMs, here using only the

Table 1. Projected Climate Changes for Glacier Regions^a

Region	T 2003–2022	T 2081–2100	ΔT	T_{summer} 2003–2022	T_{summer} 2081–2100	ΔT_{summer}	P 2003–2022	P 2081–2100	ΔP
Alaska	0.1 ± 0.3	2.4 ± 0.3	2.4 ± 0.3	9.2 ± 0.3	11.3 ± 0.3	2.1 ± 0.3	1680 ± 39	1840 ± 43	160 ± 56
Western Canada and U.S.	3.9 ± 0.3	6.0 ± 0.2	2.1 ± 0.3	13.2 ± 0.3	15.5 ± 0.3	2.3 ± 0.3	1375 ± 37	1461 ± 50	86 ± 67
Arctic Canada (North)	-17.5 ± 0.4	-14.0 ± 0.2	3.5 ± 0.4	0.4 ± 0.2	1.9 ± 0.2	1.4 ± 0.2	143 ± 6	169 ± 6	27 ± 8
Arctic Canada (South)	-13.3 ± 0.3	-10.1 ± 0.2	3.1 ± 0.3	3.0 ± 0.2	4.8 ± 0.2	1.8 ± 0.3	327 ± 9	376 ± 14	48 ± 17
Greenland	-12.6 ± 0.3	-9.9 ± 0.1	2.7 ± 0.2	1.1 ± 0.2	2.4 ± 0.2	1.4 ± 0.2	485 ± 13	557 ± 12	72 ± 15
Iceland	0.5 ± 0.3	2.4 ± 0.2	1.9 ± 0.4	5.1 ± 0.3	6.5 ± 0.2	1.3 ± 0.3	1435 ± 46	1518 ± 47	83 ± 79
Svalbard	-6.6 ± 0.5	-2.0 ± 0.3	4.6 ± 0.5	2.3 ± 0.2	4.1 ± 0.2	1.9 ± 0.2	344 ± 12	420 ± 12	76 ± 16
Scandinavia	2.6 ± 0.2	4.7 ± 0.2	2.1 ± 0.3	11.2 ± 0.2	13.0 ± 0.3	1.8 ± 0.4	1168 ± 37	1252 ± 38	84 ± 54
Russian Arctic	-10.6 ± 0.5	-5.7 ± 0.2	4.9 ± 0.5	0.8 ± 0.2	2.8 ± 0.2	2.0 ± 0.2	292 ± 11	368 ± 10	76 ± 19
North Asia	-4.1 ± 0.3	-1.6 ± 0.1	2.5 ± 0.3	12.0 ± 0.3	14.3 ± 0.2	2.3 ± 0.3	317 ± 7	344 ± 7	27 ± 9
Central Europe	7.2 ± 0.3	9.0 ± 0.2	1.8 ± 0.3	16.1 ± 0.4	18.4 ± 0.4	2.3 ± 0.5	1190 ± 34	1162 ± 48	-28 ± 55
Caucasus	7.9 ± 0.3	9.6 ± 0.2	1.7 ± 0.3	18.3 ± 0.3	20.5 ± 0.3	2.1 ± 0.4	1133 ± 40	1130 ± 32	-3 ± 59
Central Asia	-1.1 ± 0.2	1.2 ± 0.1	2.3 ± 0.2	8.8 ± 0.2	11.2 ± 0.1	2.3 ± 0.2	367 ± 8	404 ± 14	37 ± 15
South Asia (West)	-3.7 ± 0.2	-1.4 ± 0.1	2.4 ± 0.2	6.8 ± 0.3	9.1 ± 0.3	2.3 ± 0.4	669 ± 51	701 ± 66	33 ± 88
South Asia (East)	4.8 ± 0.2	6.9 ± 0.1	2.1 ± 0.2	12.4 ± 0.2	14.2 ± 0.1	1.8 ± 0.2	1414 ± 70	1567 ± 107	153 ± 129
Low Latitudes	12.2 ± 0.2	14.0 ± 0.1	1.8 ± 0.2	12.7 ± 0.2	14.4 ± 0.1	1.7 ± 0.2	937 ± 28	984 ± 25	46 ± 44
Southern Andes	5.5 ± 0.2	6.6 ± 0.1	1.1 ± 0.2	9.3 ± 0.2	10.4 ± 0.2	1.1 ± 0.2	560 ± 8	558 ± 6	-2 ± 9
New Zealand	9.5 ± 0.1	10.6 ± 0.1	1.0 ± 0.1	13.7 ± 0.2	14.6 ± 0.2	1.0 ± 0.3	1718 ± 38	1761 ± 44	43 ± 66

^aProjected mean annual near-surface air temperature (°C), summer temperature (°C), and annual precipitation (mm) for glacier regions. Numbers are multimodel means ± standard deviations from 14 GCMs with the RCP4.5 emission scenario, averaged over the indicated period and over all GCM grid cells in a region that contain glaciers, weighted by the 2003 glacier area within each cell. Summer is June–August in the Northern Hemisphere and December–February in the Southern Hemisphere.

emission scenario RCP4.5. According to this scenario, the multimodel mean temperatures are expected to increase for all glacier regions (Figure 3 and Table 1) anywhere from 1 to 5°C over the twenty-first century. The most dramatic temperature increases occur in Svalbard and Russian Arctic, showing pronounced Arctic amplification of the projected global warming. However, much of that temperature increase occurs in winter and therefore might not significantly impact glacier melt and runoff. Summer temperature increases range from 1 to 3°C. Multimodel mean precipitation is also increasing for most regions, with the remainder of regions holding steady (Caucasus and Southern Andes) or declining slightly (Central Europe, -2%). The largest percent increases for precipitation are also found in Svalbard (+22%) and Russian Arctic (+26%).

4. Results

4.1. Glacier Runoff Evolutions and Trends

Figure 4 shows the projected time series of annual glacier runoff and glacier volume, both normalized relative to their 2003–2012 means, for each of the 18 regions. The runoff projections are shown for each GCM in addition to the multimodel mean, while the volume projections are shown as a multimodel mean only. Many regions show dramatic glacier volume losses, in particular Western Canada and U.S., Scandinavia, North Asia, Central Europe, Caucasus, and Low Latitudes, all of which are projected to lose more than 75% of their current glacier volume by 2100. These results have been discussed at length in Radić *et al.* [2013] and are presented here only for reference. In terms of glacier runoff, the 18 regions exhibit a variety of responses to the projected climate scenarios. Most regions exhibit a fairly steady decline in runoff, demonstrating that they have passed their peak runoff. For example, runoff from glaciers in Western Canada and U.S. declines by 72% between 2003–2022 and 2080–2099. Low Latitudes exhibits the fastest runoff decline due to its rapid and near complete volume loss; runoff declines 96%. In some regions, runoff is stable for a few decades and then declines (by 29% in Alaska and by 25% in Arctic Canada South). Iceland, Svalbard, and South Asia West experience increasing runoff until the middle of the century, peaking 22%, 54%, and 27% higher than the initial period and declining thereafter, ending 30%, 10%, and 11% below their initial values, respectively. In Arctic Canada North and Russian Arctic, the runoff steadily increases throughout most of the twenty-first century ending 36% and 85% higher than the initial period.

To facilitate more detailed analysis of these runoff responses, we calculated linear trends in regional glacier runoff over three periods (2003–2022, 2041–2060, and 2080–2099, Figure 5). For most regions,

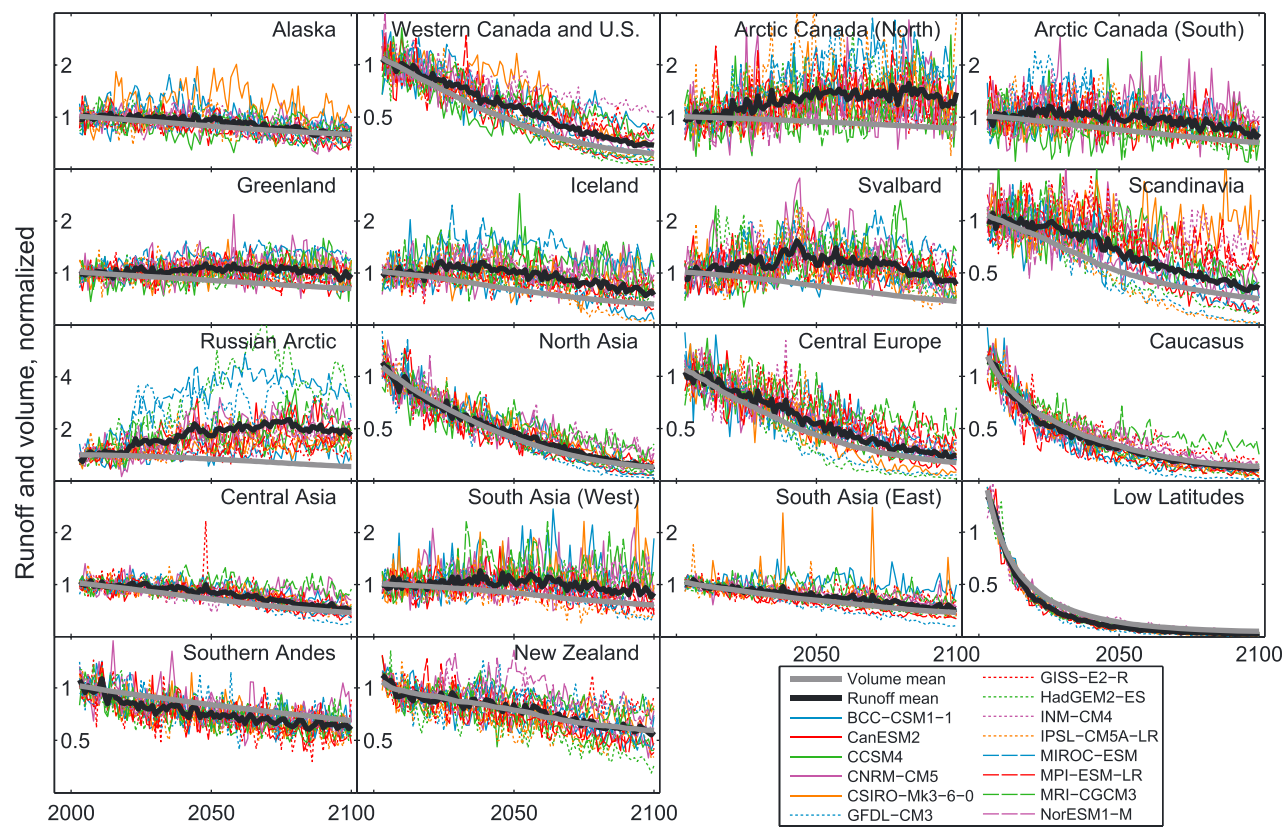


Figure 4. Projected annual glacier volume and runoff for 2003–2100 from all glaciers in each region. All lines are normalized to their mean value from 2003 to 2012. Each colored line represents the projected runoff from one global climate model and the black line is the multimodel mean. Projected volume is presented only as a multimodel mean (grey line).

Region	2003-2022		2041-2060		2080-2099	
	Trend km ³ a ⁻¹	N _{positive} %	Trend km ³ a ⁻¹	N _{positive} %	Trend km ³ a ⁻¹	N _{positive} %
Alaska	-0.090	36.2	-0.909	19.2	-1.743	5.9
Western Canada and U.S.	-0.606	24.9	-0.539	10.0	-0.318	6.7
Arctic Canada (North)	1.106	74.9	0.845	29.6	-2.070	1.6
Arctic Canada (South)	0.616	47.4	-0.142	22.4	-1.000	5.7
Greenland	0.108	68.5	0.170	55.2	-0.969	31.1
Iceland	0.120	27.6	-0.418	16.5	-0.475	22.8
Svalbard	0.702	67.7	-0.860	3.4	-0.811	2.7
Scandinavia	-0.043	28.6	-0.130	7.6	-0.062	9.9
Russian Arctic	0.997	89.7	0.300	12.9	-0.542	1.8
North Asia	-0.153	11.6	-0.057	8.7	-0.036	12.8
Central Europe	-0.093	27.0	-0.095	14.6	-0.042	8.8
Caucasus	-0.185	14.1	-0.035	10.9	-0.014	12
Central Asia	-0.153	52.9	-0.701	22.5	-0.651	9.3
South Asia (West)	0.111	61.5	0.358	50.1	-0.149	36.2
South Asia (East)	-0.687	46.7	-0.492	33.5	-0.462	18.9
Low Latitudes	-1.127	4.1	-0.072	4.2	-0.013	7.3
Southern Andes	-0.847	27.8	-0.240	26.5	-0.135	15.4
New Zealand	-0.067	28.2	-0.019	19.8	-0.013	7.9

Runoff trend (km³ a⁻¹)

-2.0 -1.5 -1.0 -0.5 0.0 0.5 1.1

Figure 5. Linear regression slopes of annual glacier runoff (multimodel mean from 14 GCMs, RCP4.5) from all glaciers in a region over three time periods. Regression slopes that are not significant at $p = 0.05$ are given in italic. Regions with opposing signs in the trend during different periods are highlighted in bold. N_{positive} is the percentage of glaciers with a positive trend (increasing runoff).

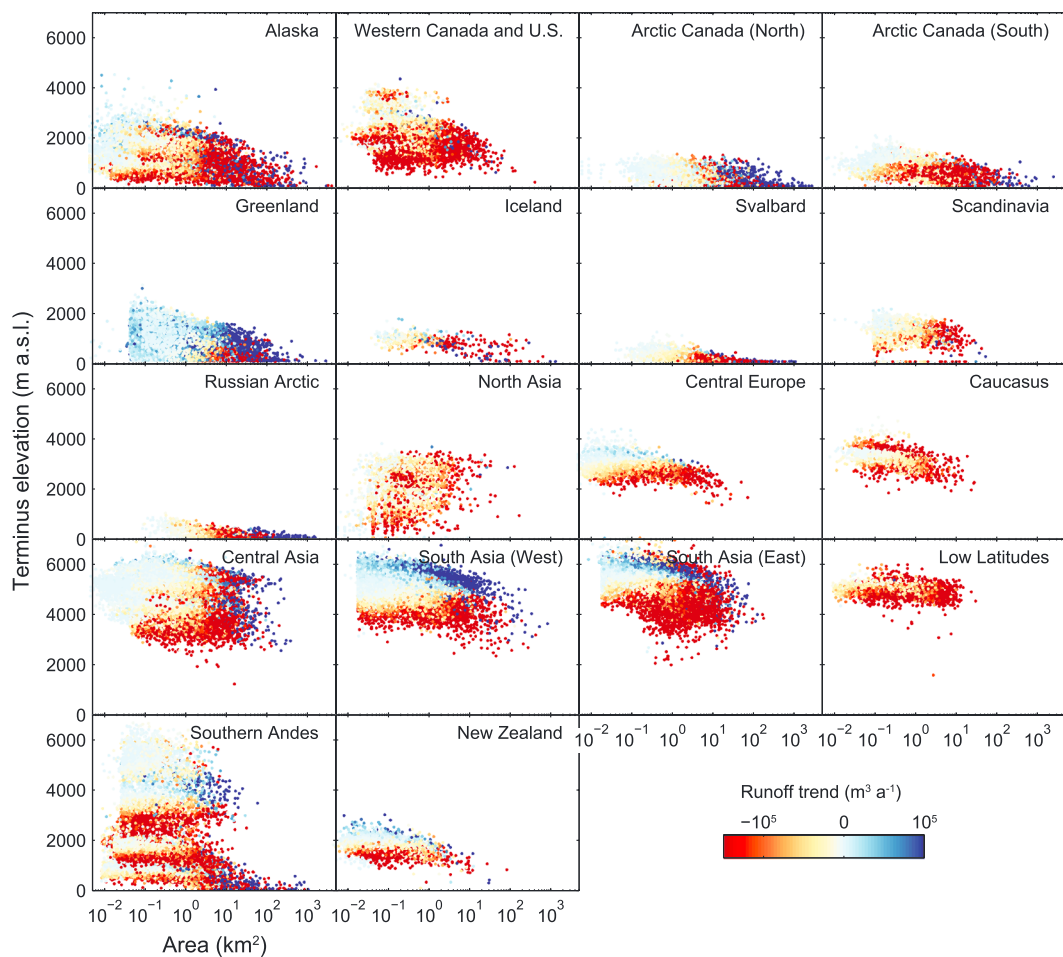


Figure 6. Runoff trends (cubic meter per annum) for each glacier versus the glacier's initial terminus elevation (y axis) and initial area (x axis). The linear trends are calculated from the annual multimodel mean runoff values from 2003 till the glacier disappears or 2100. The color scale is limited to $[-1.5 \times 10^5, 1 \times 10^5]$ to better show the data; approximately 15% of points are outside that range.

multimodel mean glacier runoff shows small negative trends (below $-0.1 \text{ km}^3 \text{ a}^{-1}$, about $-1\% \text{ a}^{-1}$) which hold relatively steady over the three periods. Other patterns follow those in Figure 4. Figure 5 also shows the percentage of glaciers within each region that have positive runoff trends. Low Latitudes has only 4% of glaciers with increasing runoff in the first period considered. Russian Arctic has the highest percentage, but over the course of the century, the percentage drops to be one of the lowest at the end of the century. All the glaciers in that region respond to climate perturbations in sync with each other.

To explore the influence of glacier size and elevation on the runoff trends, we compute the linear runoff trend of each individual glacier over the entire period 2003–2100 or until the glacier has melted away, whichever comes first. We plot the trends as a function of initial glacier size and initial terminus elevation in Figure 6. These results must be treated with caution because the model has been calibrated to mimic regional-scale mass balances rather than to accurately reproduce the evolution of individual glaciers [Radić and Hock, 2011]. Additionally, in cases where peak runoff occurs during the century, these 2003–2100 trends are sensitive to the timing of the peak. Positive runoff trends at high elevations contrast with strongly negative trends at low elevations across all size classes in many regions (best examples: Central Europe, South Asia (West and East), and New Zealand). Most regions show runoff trends that also depend on glacier size. This is to be expected because even a small percent change in a large glacier will lead to a large runoff trend. We see that small glaciers in many regions are able to have large trends due to their fast retreats and in many cases disappearance. In

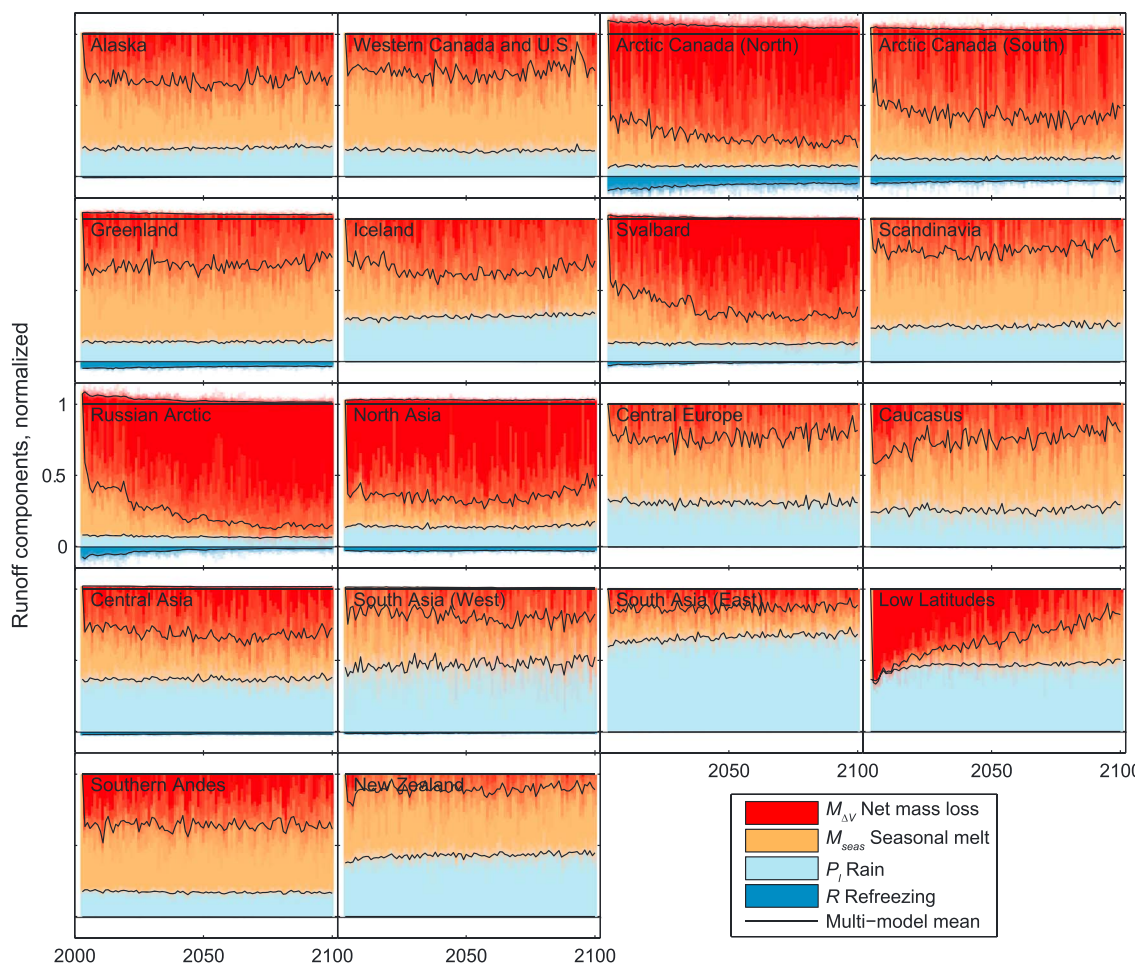


Figure 7. Runoff component time series, relative to total runoff for each year. Results from each of the 14 GCMs are plotted with high transparency so all models are visible. Black lines mark the boundaries between components for the multimodel means. In regions with refreezing, the range of the plot exceeds [0 1] but the sum of all components is equal to 1. See also Table 2.

Arctic Canada (South), Scandinavia, and Alaska, the larger glaciers tend to have more negative trends than smaller glaciers. In Greenland, the trends tend to be more positive for the smaller glaciers; however, for the larger size category (glacier area $> 100 \text{ km}^2$), both negative and positive trends are found, the former mostly from glaciers at low altitudes and the latter from glaciers at higher altitudes. Banded patterns (e.g., Alaska, Central Asia, and Southern Andes) arise for two main reasons. First, the aforementioned cases where peak runoff occurs during the century. If runoff peaks prior to the middle of the century, the overall trend will be negative, otherwise it will be positive. The second mixed pattern arises when clusters of glaciers within the region overlap with each other on the plot. The best example of this is Southern Andes, but it also appears to some extent in every region. Terminus elevations for Southern Andes glaciers between latitudes 50 to 55°S range from 0 to 1000 m and the runoff trends for glaciers terminating at sea level are negative, while those ending at 1000 m are positive. Farther north (e.g., 35–40°S), the pattern is the same, but the elevation range is 2000–3500 m due to the warmer climate.

4.2. Runoff Components

Figure 7 shows time series of runoff components (seasonal melt M_{seas} , glacier net mass loss $M_{\Delta V}$, rain on the glacier, and refreezing; equations (1)–(4)) normalized by annual total glacier runoff. Table 2 summarizes runoff components for the whole century and for three 20 year intervals for each region. When interpreting these results, bear in mind that the glacier area generally decreases with time but all components are integrated over the same decreasing area and therefore are directly comparable. Results exhibit a striking range of the components'

Table 2. Total Runoff and Runoff Components^a

Region	Q_g ($\text{km}^3 \text{a}^{-1}$)	$M_{\Delta V}$ (%)	M_{seas} (%)	P_I (%)	R (%)	Region	Q_g ($\text{km}^3 \text{a}^{-1}$)	$M_{\Delta V}$ (%)	M_{seas} (%)	P_I (%)	R (%)
Alaska 2003–2099	300	33	48	20	-1	North Asia	4	66	23	14	-3
	338	30	51	19	-1		7	62	27	14	-3
	316	36	45	20	-1		3	71	18	13	-3
	241	31	48	21	-1		1	64	24	15	-3
W. Canada and U.S.	38	26	55	19	0	Central Europe	6	23	46	31	0
	62	24	58	19	0		9	23	47	31	0
	38	30	53	18	0		5	25	45	31	0
	17	22	59	19	0		3	20	49	31	0
Arctic Canada (N)	158	78	21	7	-6	Caucasus	2	28	47	26	-1
	125	67	34	7	-8		5	33	42	25	0
	173	80	18	7	-6		2	26	50	25	-1
	170	81	16	7	-5		1	19	54	28	-1
Arctic Canada (S)	81	59	32	13	-4	Central Asia	112	33	32	37	-2
	87	52	40	13	-4		136	28	38	37	-2
	85	61	30	12	-3		117	35	30	37	-2
	65	62	29	13	-3		80	33	31	37	-2
Greenland	156	36	54	14	-4	South Asia (W)	108	20	34	47	-1
	149	37	54	14	-5		107	16	40	45	-1
	163	37	53	14	-4		115	21	33	47	-1
	151	33	56	14	-3		95	21	31	48	-1
Iceland	48	36	33	31	0	South Asia (E)	87	13	21	66	0
	51	29	41	30	0		109	13	24	63	0
	52	39	30	32	0		87	13	21	67	0
	36	34	33	33	0		65	12	20	68	0
Svalbard	80	64	25	13	-1	Low Latitudes	4	47	10	43	0
	73	51	38	13	-2		15	52	8	41	0
	93	68	21	12	-1		2	37	16	47	0
	66	68	20	13	-1		1	21	30	49	0
Scandinavia	8	22	53	25	0	Southern Andes	63	36	47	17	0
	11	21	55	24	-1		78	34	48	18	0
	8	24	52	24	0		61	36	47	17	0
	4	19	56	26	0		54	36	47	17	0
Russian Arctic	102	81	14	7	-3	New Zealand	5	11	47	43	0
	62	62	36	8	-6		6	12	48	41	0
	114	83	12	7	-2		5	12	45	43	0
	115	87	8	7	-2		4	9	47	44	0

^aAnnual average runoff Q_g , Annual glacier net mass loss $M_{\Delta V}$, seasonal melt M_{seas} , rainfall P_I , and refreezing R as a percentage of total runoff. The first row for each region is an average over the interval 2003–2099. The next three rows correspond to intervals 2003–2022, 2041–2060, and 2080–2099, respectively. See also Figure 7.

importance among regions. In most regions, glacier melt is the dominant component of glacier runoff. However, in the monsoon regions of Asia, rain contributes $37 \pm 4\%$ (Central Asia) to $66 \pm 10\%$ (South Asia East) of the total runoff (multimodel means \pm standard deviation among models for 2003–2100, Table 2). High relative contributions of rain are also found in the Low Latitudes ($43 \pm 4\%$) and in maritime regions such as New Zealand ($43 \pm 5\%$) and Iceland ($31 \pm 3\%$). Refreezing is a small but nonnegligible component for the polar regions (Arctic Canada North, $6.0 \pm 0.4\%$; Arctic Canada South, $3.5 \pm 0.6\%$; Russian Arctic, $2.5 \pm 0.6\%$; and Greenland, $3.8 \pm 0.5\%$). The relative partitioning of melt between seasonal melt and net glacier mass loss varies greatly between the regions. Seasonal melt almost entirely dominates total melt in New Zealand ($M_{\text{seas}} = 81 \pm 11\%$ of M for the multimodel mean \pm standard deviation among models for 2003–2100) and Scandinavia ($70 \pm 19\%$), both regions with strongly marine climates and therefore large accumulation rates and mass-balance amplitudes. Also in Central Europe ($66 \pm 15\%$), Caucasus ($62 \pm 12\%$), Western Canada and U.S. ($68 \pm 15\%$), and South Asia West ($63 \pm 16\%$) and East ($61 \pm 14\%$), seasonal melt is more important for annual glacier runoff than net glacier mass loss, but annual mass loss remains significant through the whole 2003–2100 period. The opposite is found for Arctic Canada North ($21 \pm 4\%$) and South ($35 \pm 9\%$), Russian Arctic ($15 \pm 5\%$), North Asia

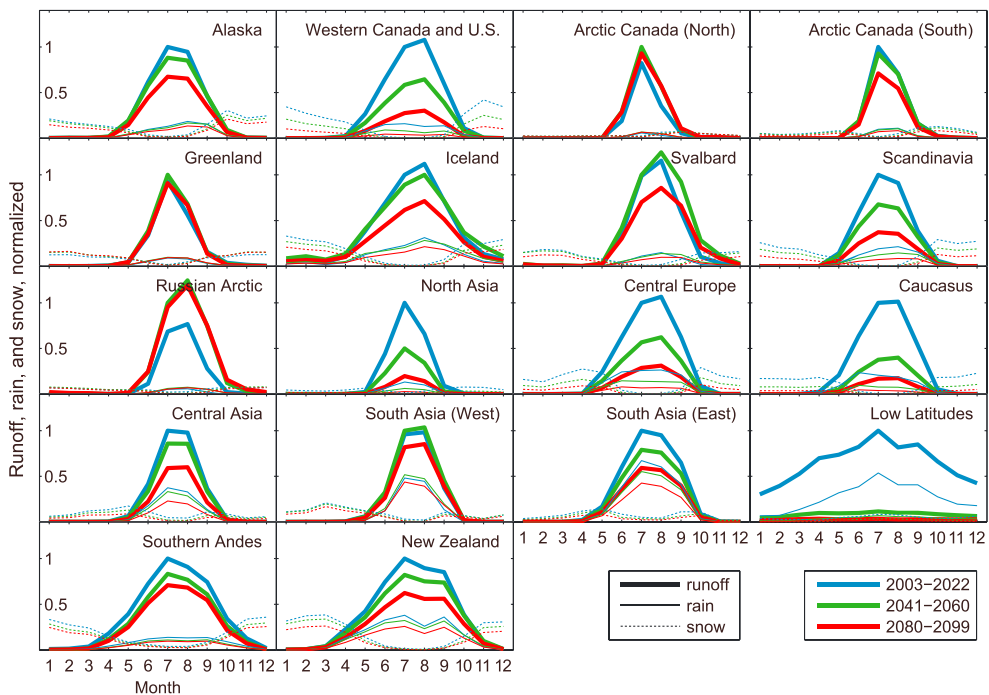


Figure 8. Monthly glacier runoff, snow accumulation, and rain averaged for three periods (2003–2022, 2041–2060, and 2080–2099). All lines represent the multi-model mean from 14 GCMs. Low Latitudes, Southern Andes, and New Zealand are shifted such that month 1 is July instead of January.

($25 \pm 7\%$), and Svalbard ($28 \pm 8\%$), regions that are characterized by relatively cold and dry high latitude climates. In these regions, net glacier mass loss dominates both total melt and glacier runoff.

In most regions, the relative importance of runoff components remains almost unchanged throughout the projection period, but some regions exhibit an increasing importance of the net mass loss component, at the expense of seasonal melt. In Arctic Canada North, net mass loss goes from $67 \pm 24\%$ of total runoff in 2003–2022 to $81 \pm 30\%$ for 2080–2099 (Table 2). Russian Arctic (62 ± 12 to $87 \pm 31\%$) and Svalbard (51 ± 17 to $68 \pm 15\%$) exhibit similar trends. In the Low Latitudes on the other hand, glacier volume change at the beginning of the century is much more important than seasonal melt ($M_{\Delta V} = 52 \pm 2\%$ of Q_g , $M_{seas} = 8 \pm 1\%$ of Q_g), but as the glacier volumes decrease to zero at the end of the century, seasonal melt becomes more important ($30 \pm 14\%$, compared to $21 \pm 6\%$ for $M_{\Delta V}$). The relative contribution of rain varies between periods by only 1 or 2% of total runoff for most regions but by up to 8% for the Low Latitudes.

4.3. Runoff Regime

Monthly glacier runoff averaged over three periods (2003–2022, 2041–2060, and 2080–2099) together with monthly rain totals and snow accumulation are shown in Figure 8. As expected, in all regions glacier runoff exhibits a strong seasonality with pronounced peaks in summer (July or August in the Northern Hemisphere and January in the Southern Hemisphere) and negligible runoff amounts in winter. Maximum monthly runoff is significantly greater than the seasonal maxima of snow accumulation or rain. Summer flows are strongly reduced from the earliest to the latest period considered.

For most regions, there is little shift in the timing of runoff from glacierized areas between each interval. This is to be expected since we only calculate the glacier runoff from each year's glacier area and not the total runoff of a glacierized catchment where the glacier may retreat but the total catchment area remains constant. In the case of a constant catchment, the disappearing glacier area will be replaced by seasonal snow cover and the loss of late-season melt from the glacier will shift the hydrograph to an earlier peak flow, as seen in unglacierized basins with winter snow that melts in late spring or early summer.

5. Discussion

Much of the controversy regarding the importance of glaciers for runoff stems from differences in defining glacier runoff [Radic and Hock, 2013]. While many studies assess the hydrological changes impacting a discharge gauging station, we choose to investigate the changes in water yields only from the glacierized area. We do not consider the runoff that results from snowmelt and rain in the deglaciated area as the glacier retreats. As a result, we are not able to assess the expected shift from a regime with late summer peak flows to a regime with progressively earlier peak flows as glacier melt declines and seasonal melt becomes dominant in driving the regime. Nevertheless, our analysis allows us to investigate characteristic patterns and differences between regions with respect to the response of glacier runoff to climate change. In addition, runoff from the glacier area has a specific physical and biogeochemical signature. Studies investigating this aspect of the hydrological response to climate change require quantification of the water yields from glaciers [Bhatia et al., 2011, 2013].

Our results show considerable differences among the regions in the response of glacier runoff to the GCM temperature and precipitation scenarios. Although some regions show considerable spread in results between the different climate scenarios, the overall patterns are consistent for each region. The regional responses result from the sum of the responses of each region's individual glaciers. All regions' glaciers show a wide range of positive and negative runoff trends, which combine to yield the regional response seen in Figure 4.

In contrast to glacier mass change, which shows consistent mass loss in all regions, region-wide glacier runoff decreases in most of the regions but increases in others (e.g., Canadian and Russian Arctic) followed by a decrease in runoff in some of these (e.g., Svalbard). These regional patterns are consistent with the expected behavior for single glaciers: glacier runoff first increases as climate progressively warms but then reaches a turning point after which glacier runoff will decrease, despite high specific melt rates, approaching zero as the glacier area (and volume) shrinks and eventually disappears [Jansson et al., 2003]. Arctic Canada North, Russian Arctic, and Greenland show significant increase in annual glacier runoff, as well as unaltered or increased summer peak flows during the twenty-first century. In the former two regions, glacier net mass loss constitutes a very large and growing proportion of total glacier runoff. While net mass loss increases due to the warming climate, the background state is still cold and dry enough to minimize the contributions of rain and seasonal melt. In addition, these regions have many large glaciers, which need more time than small glaciers to adjust their geometry to a new equilibrium. In contrast, most of the other regions have passed the turning point and show steady decline in glacier runoff indicating that the future increase in glacier runoff due to increased specific melt rates is insufficient to compensate for the future decrease in runoff due to glacier shrinkage and net mass loss. Not surprisingly, this decrease is most pronounced in regions with relatively little initial ice cover, such as Low Latitudes, Caucasus, and Central Europe.

The hydrological consequences in the High Asian Mountains due to enhanced melt have been a matter of considerable dispute [Alford and Armstrong, 2010; Immerzeel et al., 2010; Kaser et al., 2010; Bolch et al., 2012]. We find significant declines in annual glacier runoff over the twenty-first century for central Asia and South Asia East, but no significant changes for South Asia West. In these Asian regions, high relative contributions of rain to glacier runoff due to monsoon climates dampen the effect of runoff decline due to glacier decline. In addition, in South Asia West and to a lesser degree in South Asia East, increased glacier runoff due to negative trends at predominantly low-lying glaciers is at least partially compensated for by positive runoff trends of glaciers at higher altitudes. The low-lying glaciers are more vulnerable to atmospheric warming since their temperatures more readily exceed the melting temperature. They tend to lie on the declining limb of the expected glacier runoff response curve while the high-altitude glaciers have not retreated sufficiently to show a runoff decrease and tend to fall on the rising limb of the curve. We have not considered the potentially important [Scherler et al., 2011] effects of debris cover due to their uncertain magnitude and sign [Gardelle et al., 2013] and the effort that would be required to compile a global-scale glacier debris cover map.

Consistent with the strong runoff decreases, the regions with relatively low initial ice cover (e.g., Central Europe, and Caucasus) also show the most dramatic seasonal changes in glacier runoff (Figure 8) with greatly reduced summer flows by the end of the twenty-first century. Central Asia and South Asia East also show significant drops in summer peak, thus potentially impacting downstream water resources during these months. These glacier runoff reductions will be compensated to some extent by rain and snow melt runoff from formerly glacierized areas, such that at a fixed gauge downstream from the glacier, the runoff change will not be quite so dramatic.

Kaser *et al.* [2010] quantified the seasonal delays of water yields from glaciers assuming that the glaciers were in equilibrium with the local climate; i.e., any contribution to runoff from glacier net mass loss was neglected ($M_{\Delta V}=0$). Our results indicate that the glacier net mass loss is an important component of the total glacier runoff for the twenty-first century in most regions. The significance of glacier meltwater to society could thus be more important than Kaser *et al.* [2010] estimated.

6. Conclusions

We have quantified the response of twenty-first century glacier runoff from all mountain glaciers and ice caps outside Antarctic to temperature and precipitation scenarios of 14 GCMs forced with RCP4.5 emission scenario. The regional responses of 18 glacierized regions show significant differences with respect to trends in annual runoff, seasonality of runoff, and proportion of runoff derived from seasonal melt, glacier net mass loss, and rain. All regions experience significant glacier mass loss by 2100, but the magnitude and sign of trends in annual runoff totals differ considerably among regions depending on the balance between enhanced melt and the reduction of the glacier reservoir by glacier retreat and shrinkage. Most regions show strong declines in glacier runoff indicating that the effect of glacier shrinkage is more important than increased specific melt rates. Some high-latitude regions (Arctic Canada North, Russian Arctic, and Greenland) exhibit increases in runoff totals. Iceland and Svalbard show an increase in runoff followed by a multidecadal decrease in annual runoff.

Glacier runoff is dominated by snow and ice melt in most regions, but rain is an important contributor to glacier runoff in the High Asian Mountains, confirming previous studies postulating a minor role of glaciers in catchment runoff in monsoon climates. Our results emphasize the need to include the contributions from glacier net mass loss into climate impact assessments on glacier runoff.

Acknowledgments

Thanks to three reviewers for helpful comments. This study was supported by grants from NASA (NNX11AO23G, NNX11AF41G) and NSF (EAR-0943742, EAR-1039008).

References

- Adhikari, S., and S. J. Marshall (2012), Glacier volume-area relation for high-order mechanics and transient glacier states, *Geophys. Res. Lett.*, 39, L16505, doi:10.1029/2012GL052712.
- Alford, D., and R. Armstrong (2010), The role of glaciers in stream flow from the Nepal Himalaya, *Cryosphere Discuss.*, 4, 469–94.
- Arendt, A., et al. (2012), Randolph Glacier Inventory: A Dataset of Global Glacier Outlines Version: 2.0, 11 June 2012, GLIMS Technical Report.
- Bahr, D. B., M. F. Meier, and S. D. Peckham (1997), The physical basis of glacier volume-area scaling, *J. Geophys. Res.*, 102(B9), 20,355–20,362.
- Beck, C., J. Grieser, and B. Rudolf (2005), A new monthly precipitation climatology for the global land areas for the period 1951 to 2000, Published in *Climate Status Report 2004*, pp. 181–190, German Weather Service, Offenbach, Germany.
- Bhatia, M. P., S. B. Das, E. B. Kujawinski, P. Henderson, A. Burke, and M. A. Charette (2011), Seasonal evolution of water contributions to discharge from a Greenland outlet glacier: Insight from a new isotope-mixing model, *J. Glaciol.*, 57(205), 929–941.
- Bhatia, M. P., E. B. Kujawinski, S. B. Das, C. F. Breier, P. B. Henderson, and M. A. Charette (2013), Greenland meltwater as a significant and potentially bioavailable source of iron to the ocean, *Nat. Geosci.*, 6, 274–278, doi:10.1038/ngeo1746.
- Bolch, T., et al. (2012), The state and fate of Himalayan glaciers, *Science*, 336, 310–314.
- Cogley, J. G. (2009), Geodetic and direct mass-balance measurements: Comparison and joint analysis, *Ann. Glaciol.*, 50(50), 96–100.
- Comeau, L. E. L., A. Pietroniro, and M. N. Demuth (2009), Glacier contribution to the North and South Saskatchewan Rivers, *Hydro. Processes*, 23, 2640–2653, doi:10.1002/hyp.7409.
- Dyurgerov, M. B. (2010), Reanalysis of glacier changes: From the IGY to the IPY, 1960–2008, *Data Glaciol. Studies*, 108, 1–116.
- Farinotti, D., S. Usselmann, M. Huss, A. Bauder, and M. Funk (2012), Runoff evolution in the Swiss Alps: Projections for selected high-alpine catchments based on ENSEMBLES scenarios, *Hydro. Processes*, 26, 1909–1924.
- Gardelle, J., E. Berthier, Y. Arnaud, and A. Kääb (2013), Region-wide glacier mass balances over the Pamir-Karakoram-Himalaya during 1999–2011, *Cryosphere*, 7, 1263–1286, doi:10.5194/tc-7-1263-2013.
- Gardner, A., et al. (2013), A reconciled estimate of glacier contributions to sea level rise: 2003 to 2009, *Science*, 340(6134), 852–857, doi:10.1126/science.1234532.
- Giesen, R. H., and J. Oerlemans (2013), Climate-model induced differences in the 21st century global and regional glacier contributions to sea-level rise, *Clim. Dyn.*, doi:10.1007/s00382-013-1743-7.
- Hock, R., P. Jansson, and L. Braun (2005), Modelling the response of mountain glacier discharge to climate warming, in *Global Change and Mountain Regions—A State of Knowledge Overview*, edited by U. M. Huber, M. A. Reasoner, and H. Bugmann, pp. 243–252, Springer, Dordrecht.
- Hood, E., and L. Berner (2009), The effect of changing glacial coverage on the physical and biogeochemical properties of coastal streams in southeastern Alaska, *J. Geophys. Res.*, 114, G03001, doi:10.1029/2009JG000971.
- Huss, M. (2011), Present and future contribution of glacier storage change to runoff from macroscale drainage basins in Europe, *Water Resour. Res.*, 47, W07511, doi:10.1029/2010WR010299.
- Huss, M., D. Farinotti, A. Bauder, and M. Funk (2008), Modelling runoff from highly glacierized alpine drainage basins in a changing climate, *Hydro. Processes*, 22, 3888–3902, doi:10.1002/hyp.7055.
- Immerzeel, W. W., L. P. H. van Beek, and M. F. P. Bierkens (2010), Climate change will affect the Asian water towers, *Science*, 328, 1382, doi:10.1126/science.1183188.
- Jansson, P., R. Hock, and T. Schneider (2003), The concept of glacier water storage—A review, *J. Hydrol.*, 282(1–4), 116–129, doi:10.1016/S0022-1694(03)00258-0.
- Kaser, G., M. Grosshauser, and B. Marzeion (2010), Contribution potential of glaciers to water availability in different climate regimes, *Proc. Natl. Acad. Sci.*, 107, 20,223–20,227, doi:10.1073/pnas.1008162107.

- Koboltschnig, G. R., W. Schoner, M. Zappa, C. Kroisleitner, and H. Holzmann (2008), Runoff modelling of the glacierized Alpine Upper Salzach basin (Austria): Multi-criteria result validation, *Hydrol. Processes*, 22, 3950–3964, doi:10.1002/hyp.7112.
- Marzeion, B., A. H. Jarosch, and M. Hofer (2012), Past and future sea-level change from the surface mass balance of glaciers, *Cryosphere*, 6, 1295–1322, doi:10.5194/tc-6-1295-2012.
- Meier, M., M. Dyurgerov, U. Rick, S. O'Neal, W. Pfeffer, R. Anderson, S. Anderson, and A. Glazovsky (2007), Glaciers dominate eustatic sea-level rise in the 21st century, *Science*, 317, 1064.
- Moss, R. H., et al. (2010), The next generation of scenarios for climate change research and assessment, *Nature*, 463, 747–756, doi:10.1038/nature08823.
- Neal, E. G., E. Hood, and K. Smikrud (2010), Contribution of glacier runoff to freshwater discharge into the Gulf of Alaska, *Geophys. Res. Lett.*, 37, L06404, doi:10.1029/2010GL042385.
- Radić, V., and R. Hock (2006), Modeling future glacier mass balance and volume changes using ERA-40 reanalysis and climate models: A sensitivity study at Storglaciären, Sweden, *J. Geophys. Res.*, 111, F03003, doi:10.1029/2005JF000440.
- Radić, V., and R. Hock (2011), Regional differentiated contribution of mountain glaciers and ice caps to future sea-level rise, *Nat. Geosci.*, 4, 91–94, doi:10.1038/NGEO1052.
- Radić, V., and R. Hock (2013), Glaciers in the Earth's hydrological cycle: Assessments of glacier mass and runoff changes on global and regional scales, *Surv. Geophys.*, 1–25, doi:10.1007/s10712-013-9262-y.
- Radić, V., R. Hock, and J. Oerlemans (2008), Analysis of scaling methods in deriving future volume evolutions of valley glaciers, *J. Glaciol.*, 54, 601–612, doi:10.3189/002214308786570809.
- Radić, V., A. Bliss, A. C. Beedlow, R. Hock, E. Miles, and J. G. Cogley (2013), Regional and global projections of 21st century glacier mass changes in response to climate scenarios from global climate models, *Clim. Dyn.*, doi:10.1007/s00382-013-1719-7.
- Robinson, C. T., U. Uehlinger, and M. Hieber (2001), Spatio-temporal variation in macroinvertebrate assemblages of glacial streams in the Swiss Alps, *Freshwater Biol.*, 46, 1663–1672, doi:10.1046/j.1365-2427.2001.00851.x.
- Scherler, D., B. Bookhagen, and M. Strecker (2011), Spatially variable response of Himalayan glaciers to climate change affected by debris cover, *Nat. Geosci.*, 4, 156–159.
- Stahl, K., R. D. Moore, J. M. Shea, D. Hutchinson, and A. J. Cannon (2008), Coupled modelling of glacier and streamflow response to future climate scenarios, *Water Resour. Res.*, 44, W02422, doi:10.1029/2007WR005956.
- Weber, M., L. Braun, W. Mauser, and M. Prasch (2010), Contribution of rain, snow and icemelt in the upper Danube today and in the future, *Geogr. Fis. Din. Quat.*, 33, 221–230.
- Woodward, J., M. Sharp, and A. Arendt (1997), The influence of superimposed-ice formation on the sensitivity of glacier mass balance to climate change, *Ann. Glaciol.*, 24, 186–190.